IEEE Access
Multidisciplinary | Rapid Review | Open Access Journal

Received March 22, 2018, accepted April 7, 2018, date of publication April 19, 2018, date of current version June 26, 2018.

*Digital Object Identifier 10.1109/ACCESS.2018.2826923*

# A Comprehensive Strategy for Power Quality Improvement of Multi-Inverter-Based Microgrid With Mixed Loads

**HENAN DONG[1,2,3], SHUN YUAN[1,4], ZIJIAO HAN[5], XIYING DING[1], SHAOHUA MA[1], AND XIANGYU HAN[1]**

[1]Institute of Electrical Engineering, Shenyang University of Technology, Shenyang 110023, China
[2]Liaoning Electric Power Company Electric Power Research Institute, State Grid Corporation of China, Shenyang 110006, China
[3]Liaoning Dongke Electric Power Company, State Grid Corporation of China, Shenyang, China
[4]National Energy Administration, Beijing 100085, China
[5]Liaoning Electric Power Company, State Grid Corporation of China, Shenyang 110004, China

Corresponding author: Shaohua Ma (mash_dq@sut.edu.cn)

This work was supported in part by the National Science and Technology Support Project of China under Grant 2015BAA01B2 and in part by Liaoning Electric Power Co., Ltd. Science and Technology Project of State Grid under Grant 2017YF-31.

**ABSTRACT** In order to solve the influence of nonlinear and unbalanced mixed loads on output voltage of microsource inverters in microgrid, this paper proposes a comprehensive strategy which can be used to accurate power distribution, harmonic suppression, negative-sequence voltage component suppression, and stability improvement. On one hand, a fundamental control strategy is proposed upon the conventional droop control; the problem of accurate reactive power distribution is solved by introducing virtual impedance to inverters, while considering the aggravating problem of stability because of introducing virtual impedance, a secondary power balance controller is added to improve the stability of voltage and frequency. On the other hand, the fractional frequency harmonic control strategy and negative-sequence voltage control strategy are proposed to solve the influence of mixed loads, which focus on eliminating specific harmonics caused by the nonlinear loads and the negative sequence component of the voltage. The power quality of microgrid can be improved effectively. Finally, small signal analysis is used to analyze the stability of the multiconverter parallel system after introducing the whole control strategy. The simulation results show that the strategy proposed in this paper has a great performance on distributing reactive power, regulating and eliminating harmonic components, eliminating negative-sequence components and stabilizing output voltage of inverters and frequency, and improving the power quality of multiinverter-based microgrid.

**INDEX TERMS** Microgrid, mixed loads, power quality, harmonic suppression, negative sequence voltage.

## I. INTRODUCTION

With the increase of energy demands, it is becoming an inevitable trend to make full use of distributed generations (DGs), since they have substantial advantages such as power loss reduction, greenhouse gas emission reduction, flexible voltage regulation, peak-load shaving, higher power quality, supply reliability enhancement compared with traditional centralized generations [1]. Large-scale distributed power supply interconnection makes microgrid, which can be used as a powerful supplement and effective support for large power grid. There is no doubt that this kind of distributed generation interconnection of microgrid will be one of the trends of power system development [2]. It is worth noting that the safe and reliable operation of microgrid with distributed energy is an important prerequisite. However, the microgrid is close to the load and is easily affected by the load. The increase of unbalanced load and nonlinear load will have an impact on the power quality of the whole microgrid. In severe cases, it can lead to the collapse of the microgrid system itself and influence the voltage and frequency of the distribution network [3].

The micro-source inverter plays a very important role in microgrid. As distributed generations are connected to microgrid via inverter, the control strategy of inverters will influence on system stability and power quality. Among all the inverter control strategies, droop control is considered as the best strategy at present [4], which can distribute the output power of inverters properly under island mode of

microgrid, even there is no common communication line among DGs, meanwhile, the voltage and frequency can be controlled within related national standards by this strategy. However, there are some shortages in conventional droop control strategy. Firstly, system reactive power cannot be distributed accurately while equivalent impedance of micro sources is different. Secondly, there are no suppression measures for harmonic and the voltage negative sequence components under traditional droop control. The magnitude of harmonic power varies with the amount of non-linear loads integrated into microgrid. The existence of harmonic power will have an effect on system devices, including transformers, capacitors and electric rotating machines. Unbalanced load directly affects the stability of the system, which may cause damage of power electronics equipment in the microgrid [5].

There is a voltage and current double-loop control strategy for inverter [6], which takes advantage of the inner current loop to improve inverter dynamic performance. The repetitive control theory and PID control strategy are combined to improve static and dynamic performance of inverters, but they lead to a considerably complex system [7]. The virtual impedance technique was introduced to a UPS parallel system to realize current sharing control [8]. By increasing a virtual inductance control loop upon the output voltage and inductance current double loop controller, the control accuracy and current sharing performance of UPS parallel system were improved, while with the consideration of the load type, the nonlinear load may have an effect on conventional virtual impedance control performance. In [9], by transforming to $\alpha\beta$ coordinate system, the fundamental and harmonic components were convenient for PI and PR control respectively, then the combination of these series of currents was set as the reference signal of inverter output voltage. While the harmonic suppression effects may unsatisfactory when the current waveforms were in serious distortion. On the basis of symmetrical components theory, Dan *et al.* [10] analyzed a system with unbalanced load, and proposed a control scheme which is the combination of fundamental disturbance instantaneous value feedback PI controller and harmonic repetitive controller, though the output voltage was high qualified, the PI controller cannot eliminate dynamic error and repetitive control, and the repetitive controller just has the ability to regulate the recur distortions. A three-dimensional space vector pulse width modulation strategy was proposed in [11] and [12], which was merely effective when the unbalanced degree of load was slight. In fact, by increasing an observer and a predicter before the voltage loop, the control effect was similar [13]. A robust distributed voltage control strategy was proposed to suppress unbalanced load and specific harmonic components, while its ability of elimination is limited [14]. The resonance controller was used to solve the problem carried by unbalanced or harmonic linear load, which was complex and with low calculation rate [15]. In [16], a control strategy which combines double loop structure and internal model control is proposed. This method is a better solution for nonlinear load, and has little effect on unbalanced load. In addition, the paper only analyzes the single-phase situation, and the power is low. It is necessary to explore further the measures to reduce the harmonics in large power. In [17], the relationship between amplitudes of the active power oscillations and the reactive power oscillations resulting from unbalanced grid voltage conditions has been deduced for the first time and the hierarchical control of DG is proposed to reduce power oscillations, which provides a new way for addressing such challenges. Simulation results show that the proposed control scheme with less injecting negative-sequence current than traditional control methods can effectively limit both active power and reactive power oscillations. It proposed in [18] that the three-phase four-bridge arm inverter topology can eliminate zero sequence component distortion, but the switching frequency is low, and the regulation bandwidth is limited, which is not suitable for the input and output of the inverter with electrical isolation. In [19], a control strategy for power quality improvement under mixed loads is proposed. This control strategy adds many harmonic compensation and negative sequence unbalance compensation under the fundamental wave control strategy, which can improve the power quality, but the article only analyzes the single inverter, and does not explore the parallel characteristics of multiple inverters. A three-phase unbalanced compensation control strategy based on improved sigmoid P-f droop control is proposed by Biying *et al.* [20] and Qunhai and Ningning [21], which is controlled by each phase individually, but the inverter structure is complex, and the three-phase circuit is coupled by the transformer common ground wire.

This paper proposes a comprehensive strategy for accurate power distribution, harmonic suppression, negative sequence voltage component suppression, and stability improvement of multi-inverter-based microgrid, since the output voltage and frequency of microgrid are all consist of fundamental, harmonic and negative sequence components, the strategy contains two parts accordingly. On one hand, a fundamental control strategy is proposed upon the conventional droop control, the problem of accurate reactive power distribution is solved by introducing virtual impedance to inverters, while considering the aggravating problem of stability because of introducing virtual impedance, a secondary power balance controller is added to improve the stability of voltage and frequency. On the other hand, the fractional frequency harmonic control strategy and negative sequence component are proposed to solve the influence of nonlinear loads and unbalanced loads, microgrid inverters and the distribution network on output voltage of inverters, which are focus on eliminating specific harmonics caused by the nonlinear loads and negative sequence component by unbalanced loads, microgrid converters and the distribution network, so the power quality of microgrid can be improved effectively. Finally, small signal analysis is used to analyze the stability of the multi-converter parallel system after introducing the whole control strategy. Above all, this paper proposes a comprehensive strategy which aims at improving the power quality of

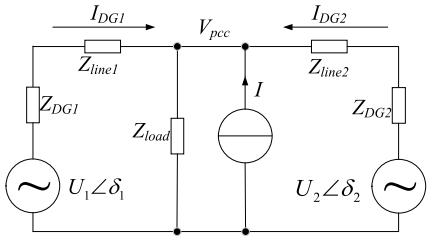


**FIGURE 1.** Circuit of a multi-inverter-based microgrid system.

microgrid further. The novelty of the proposed approach mainly lies in two-folds: the fundamental control strategy is improved by adding adaptive virtual impedance and secondary power balance control strategies; what's more, the harmonics and unbalance components of microgrid are suppressed by adding fractional frequency harmonic and negative sequence components suppression strategy. In addition, the stability of this microgrid control system is analyzed by small signal analysis method. Following this, a micro-gird system simulation model is built in RTLAB to verify the effectiveness of the proposed strategy.

The paper is organized as follows. Section2 introduces the method to model the multi-inverter-based microgrid system. Section3 proposes the comprehensive strategy for accurate power distribution, stability improvement and harmonic suppression of multi-inverter-based microgrid. Section4 analyzes the stability of the multi-converter parallel system after introducing the comprehensive control strategy. Simulation and experimental results to prove the effectiveness of the strategy are demonstrated in Section 5. Section6 concludes the paper.

## II. INTRODUCTION OF A MULTI-INVERTER-BASED MICROGRID SYSTEM

### A. CIRCUIT OF A MULTI-INVERTER-BASED MICROGRID SYSTEM

There are two inverters in classical multi-inverter-based microgrid system, which are paralleled to supply power to the common load through line impedances, the mathematical model of the system can be illustrated as shown in Fig. 1, where each inverter is modeled as a reference voltage with an output impedance, and the load is modeled as a current source or combinations of voltage and current sources.

### B. INTRODUCTION OF A CONVENTIONAL DROOP CONTROLLER

The schematic diagram of droop control of inverter shown in Fig. 2. Droop controller is an important part of inverter droop control.

In conventional droop control, droop controllers calculate frequency and voltage magnitude on the basis of micro sources droop characteristic curve, and then the reference voltage $U_{ref}$ is acquired, next the output voltage of each inverter will track its reference voltage by double closed-loop

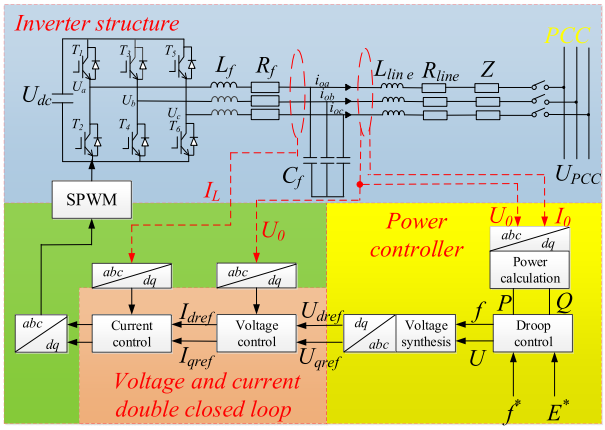


**FIGURE 2.** Inverter droop control block diagram.

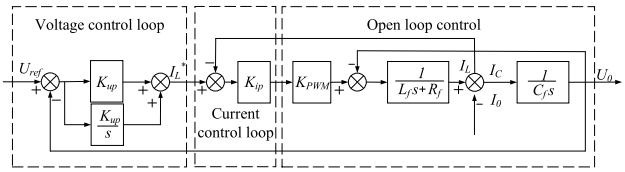


**FIGURE 3.** Double closed loop structure diagram of voltage and current.

feedback voltage-source controller. The double closed-loop feedback voltage-source controller is shown as Fig. 3.

In a microgrid with nonlinear loads, conventional droop control can be used to achieve the accurate distribution of active power. The traditional frequency and voltage droop controller is shown in (1):

$$\begin{cases} f_{droopi} = f_i^* - m_i(P - P_i^*) \\ U_{droopi} = U_i^* - n_i(Q - Q_i^*) \end{cases} \tag{1}$$

where $f_i^*$ and $f_{droopi}$ are reference and instructive frequency; $U_i^*$ and $U_{droopi}$ are reference and instructive voltage; $m_i$ and $n_i$ are coefficients of droop control; $P$ and $Q$ are average active and reactive power after filtering; $P_i^*$ and $Q_i^*$ are rate active and reactive power.

Though active power can be accurately distributed under steady state by conventional droop control, the equivalent impedance differences will lead to reactive power distribution problem. There is an effective method to solve such problem by introducing virtual impedance into reference signal, which can be shown as (2):

$$V_{ref} = V_{droop} - Z_v i \tag{2}$$

### C. THE MECHANISM OF HARMONIC PRODUCTION IN MICROGRID

While there are nonlinear loads in microgrid, the output current of inverter will include fundamental and harmonic components, which is represented as $i_{of}$ and $i_{oh}$ respectively, then the inverter output voltage is:

$$U_0 = G_V(s)U_{ref} - Z_{of}(s)i_{of} - Z_{oh}(s)i_{oh} \tag{3}$$

where

$$G_V(s) = \frac{G_U(s)\,K_{ip}K_{PWM}}{s^2L_fC_f + [r_fc_f + K_{ip}K_{PWM}]s + G_U(s)K_{ip}K_{PWM} + 1} \tag{4}$$

$$G_U(s) = K_{up} + \frac{K_{up}}{s} \tag{5}$$

$$Z_{of}(s) = \frac{sL_f + r_f + K_{ip}K_{PWM}}{s^2L_fC_f + [r_fc + K_{ip}K_{PWM}]s + G_U(s)K_{ip}K_{PWM} + 1} \tag{6}$$

Where $G_V(s)$ is voltage gain, $G_U$(s) is voltage loop proportional gain; $Z_{of}(s)$ and $Z_{oh}(s)$ are fundamental and harmonic equivalent impedance with the same mathematical expression.

Since formula (3) neglects the harmonic components, so there are no harmonic components in reference voltage, when considering non-linear loads, it may lead to inverter output voltage distortion, the Total Harmonic Distortion (THD) will be deteriorate as well. In GB-T 15549-1993 ''Power quality Harmonics in public supply network'', it can be seen that THD values of 220 kV and 110 kV do not exceed 2%, THD values of 35 kV and 66 kV do not exceed 3.0%, THD values of 10 kV and 6 kV do not exceed 4%, THD values of 0.38 kV do not exceed 2%.

### D. THE MECHANISM OF UNBALANCE OF THREE-PHASE VOLTAGE IN MICROGRID

While there are unbalance loads in microgrid, the three-phase voltage of the microgrid is presented asymmetrically. The asymmetrical three-phase voltage can be decomposed into positive sequence component, negative sequence component, and zero sequence component by symmetrical component method. There is a positive sequence component with the forward rotation of the synchronous rotational speed $\omega_0$ and the negative sequence component with the contrarotation of the synchronous rotational speed $-\omega_0$. It is worth noting that there is no zero-sequence component in the system if no zero-sequence path.

The voltage at PCC in the $\alpha - \beta$ coordinate system is expressed as (7):

$$E_{\alpha\beta} = e^{j\omega}E^+_{dq+} + e^{-j\omega}E^-_{dq-} \tag{7}$$

where:

$$\begin{cases} E^+_{dq+} = E^+_{d+} + jE^+_{q+} \\ E^-_{dq-} = E^-_{d-} + jE^+_{q-} \end{cases} \tag{8}$$

In (8), the superscript represents positive and negative sequence components; the subscript represents a positive and negative direction synchronous rotating coordinate system.

The three-phase voltage unbalance factor is used to measure the degree of the three-phase voltage deviation, which is the ratio of the negative sequence component to the positive sequence component. It will affect the normal operation of the microgrid if the three-phase voltage is not balanced, and unable to meet user needs. In GB-T 15543-2008 ''Power quality Three-voltage unbalance'', it can be seen that the negative sequence voltage unbalance caused by the user does not exceed 1.3% for a short time, and does not exceed 2.6% for a long time. Normally, the negative sequence voltage unbalance of the PCC does not exceed 2.0% for a short time, and does not exceed 4.0% for a long time.

## III. COMPREHENSIVE STRATEGY FOR ACCURATE REACTIVE POWER DISTRIBUTION, HARMONIC SUPPRESSION, NEGATIVE SEQUENCE VOLTAGE SUPPRESSION AND STABILITY IMPROVEMENT OF MULTI-INVERTER-BASED MICROGRID

It is difficult to accurately distribute reactive power and effectively improve the stability of voltage and frequency under abrupt load variation depending on conventional droop controllers, let alone suppress harmonic components in microgrid which caused by many reasons. Therefore, a comprehensive strategy for accurately distributing reactive power, improving stability and suppressing harmonic of multi-inverter-based microgrid is proposed in this paper. Upon conventional droop control, an adaptive virtual impedance control loop is introduced to achieve the accurate distribution of reactive power of inverters in fundamental frequency, considering this process may add the problem of voltage stability, a secondary balance controller is added to improve the stability of voltage and frequency, the fundamental problems are settled completely so far. Next, the control strategy this paper proposed is further refined by introducing fractional frequency harmonic suppression strategy, which can solve the harmonic problem perfectly, therefore, the power quality of microgrid is improved eventually. The main control block diagram is shown in Fig. 4.

In Fig. 4, $L_f$ is the filter inductance; $R_f$ is the filter resistance; $C_f$ is the filter capacitance; $R_{line}$ is the line resistance; $L_{line}$ is the line inductance; $R_{ref}$ is the reference resistance; $X_{ref}$ is the reference reactance; $R_i$ is the calculated value of line resistance, $X_i$ is the calculated value of line inductance; $P_{line}$ is the line active power; $Q_{line}$ is the line reactive power; $P_{i_LPF}$ is the active power that passes through the low pass filter; $Q_{i_LPF}$ is the reactive power that passes through the low pass filter; $E^*$ is an reference voltage; $f^*$ is an reference frequency; $E_{nh}$ is the *nth* harmonic voltage; $P_{nh}$ is the active power of the *nth* harmonic; $Q_{nh}$ is the reactive power of the *nth* harmonic.

### A. FUNDAMENTAL WAVE ADAPTIVE VIRTUAL IMPEDANCE DROOPING CONTROL STRATEGY

In order to achieve accurate distribution of reactive power of inverters, an adaptive virtual impedance control loop is introduced upon conventional droop control. The control block diagram is shown in Fig. 5.

The output voltage function of the inverter with virtual impedance is

$$U_0(s) = G(s)U_{ref}(s) - \left[G(s)Z_v(s) + Z_{eq}(s)\right]I_0(s) \tag{9}$$

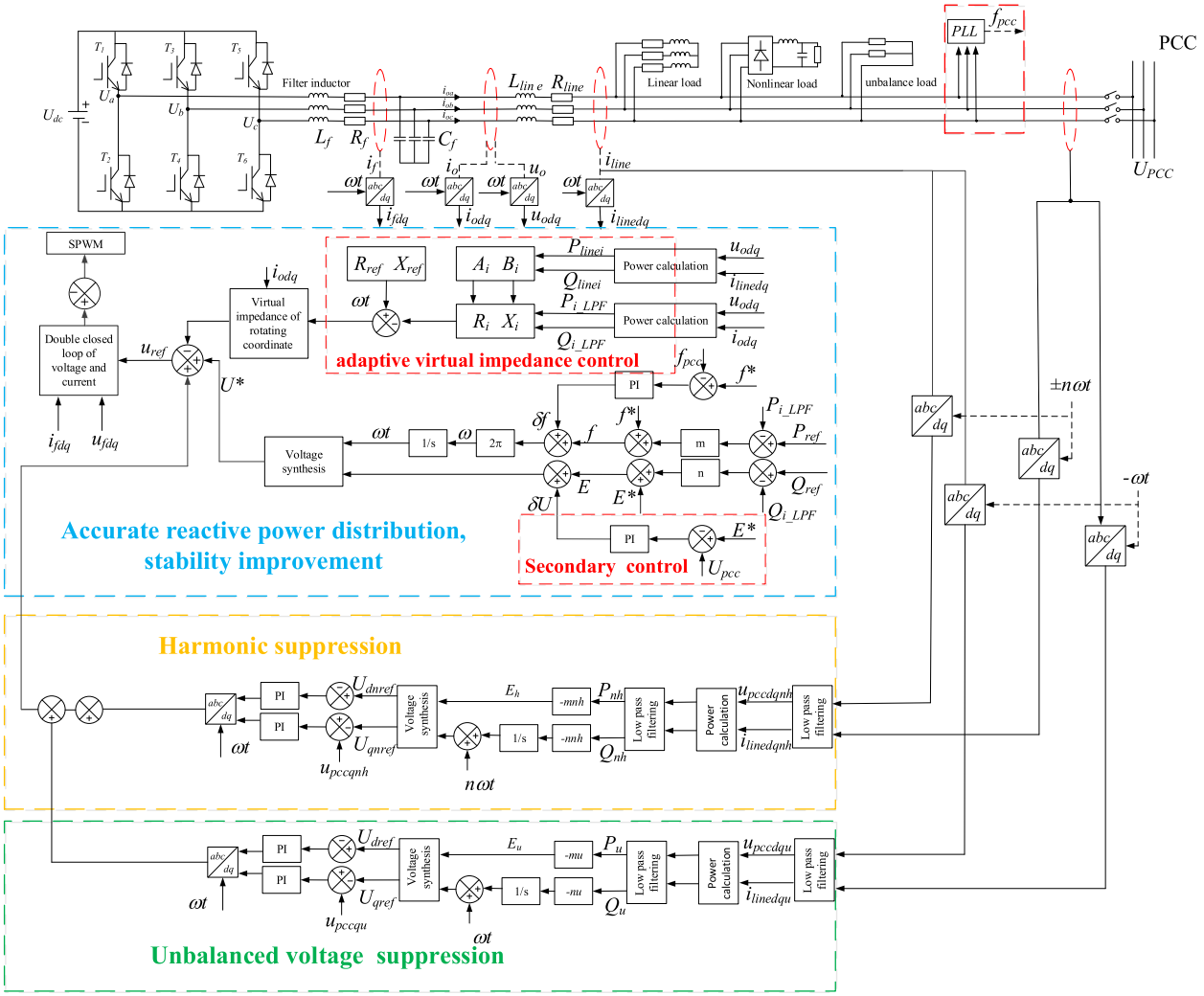


**FIGURE 4.** Block diagram of master control strategy.

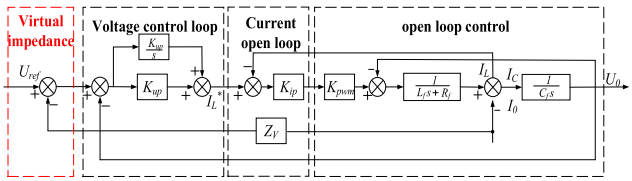


**FIGURE 5.** Inverter control block diagram with virtual impedance.

The outpower values of the inverter can be calculated by

$$P_i = \frac{U_i}{R_i^2 + X_i^2}\left[R_i(U_i - Ecos\delta_i) + X_i Esin\delta_i\right] \quad (10)$$

$$Q_i = \frac{U_i}{R_i^2 + X_i^2}\left[-R_i Esin\delta_i + X_i(U_i - Ecos\delta_i)\right] \quad (11)$$

Where $R_i$ and $X_i$ are the power equivalent output resistance and reactance, which is defined by inverter output power and the power injected to the PCC.

Based on the above circuit, the transmission line parameters and loads fluctuation will effect the value of power equivalent impedance, then influence the reactive power distribution. The power equivalent impedance can be calculated through line power.

$$U_i(U_i - Ucos\delta_i) = P_{linei}R_{linei} + Q_{linei}X_{linei} = A_i \quad (12)$$

$$U_i Usin\delta_i = P_{linei}X_{linei} - Q_{linei}R_{linei} = B_i \quad (13)$$

And the inverter equivalent output impedance can be obtained by

$$R_i = \frac{P_i A_i + Q_i B_i}{P_i^2 + Q_i^2} \quad (14)$$

$$X_i = \frac{P_i B_i - Q_i A_i}{P_i^2 + Q_i^2} \quad (15)$$

Then the virtual impedance of each micro source is calculated by:

$$R_{vi} = R_{ref} - R_i \quad (16)$$

$$X_{vi} = X_{ref} - X_i \quad (17)$$

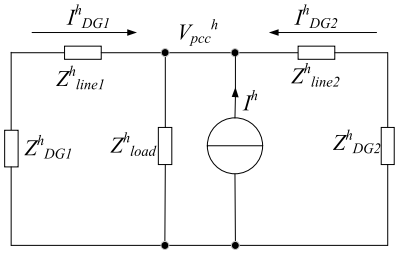


**FIGURE 6.** System equivalent circuit containing different frequencies.

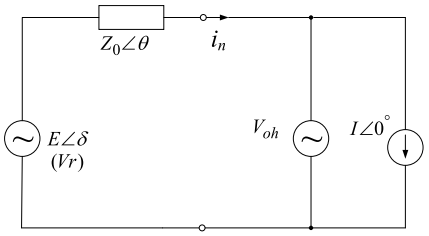


**FIGURE 7.** Single-Inverter System Equivalent Diagram.

where $R_{ref}$, $X_{ref}$ stand for reference impedance, which meeting the impedance matching relationship, in addition to, the reference impedance should reduce the line resistance and enhance the circuit inductance, so it is desirable:

$$R_{ref} = \min(R_i) X_{ref} = \max(X_i)$$

According to the formula (12)—(17), the adaptive virtual impedance control strategy can accurately distribute reactive power, meeting the requirement of the power decoupling and stability margin. More importantly, it not only can make the power equivalent impedance $R_i, X_i$ adapt the change of the local load, but also can adjust the reference impedance $R_{ref}$, $X_{ref}$ through the microgrid central controller, according to the actual operating conditions and operating parameters to meet the decoupling and stability margin of the micro-source power.

The line impedance parameters $R_{linei}, X_{linei}$ will be identified respectively with RLS (Recursive Least Square). At the same time, due to the information transmission requirements of the existing power grid, the low-speed communication line is used to collect grid bus information, and the line impedance parameters is calculated to complete the adaptive virtual impedance calculation.

### B. FRACTIONAL FREQUENCY HARMONIC DROOPING CONTROL STRATEGY

According to the circuit superposition theorem, a linear circuit with different frequencies can be analyzed separately at each frequency. Tu *et al.* [22] confirmed that any harmonic, e.g., the *hth* harmonic can be extracted for separate analysis and control when the whole system enters steady state, so the harmonic droop control strategy is proposed to eliminate the 5th, 7th harmonics generated by nonlinear loads. In order to reduce the harmonic voltage of the system, the harmonic voltage compensation value is calculated by the harmonic droop control strategy. The system equivalent schematic is shown in Fig. 6.

Single-Inverter System Equivalent Diagram is shown in Fig. 7.

then the output voltage of inverter can be obtained:

$$\begin{aligned}\bar{V}_o &= E\angle\delta - Z_o I\angle\theta \\ &= E\cos\delta - Z_o I\cos\theta + j\left(E\sin\delta - Z_o I\sin\theta\right)\end{aligned} \tag{18}$$

The phase angle difference $\delta$ is the phase angle difference between the voltage source and the current source, when it is very small, (19) and (20) can be obtained:

$$P \approx EI - Z_o I^2\cos\theta \tag{19}$$

$$Q \approx EI\delta - Z_o I^2\sin\theta \tag{20}$$

From (19) and (20), it can be found that whether the impedance of the line is inductive, resistive or capacitive, the correlation between $P$ and $E$, $Q$ and $\delta$ can be concluded. Thus, the *hth* harmonic droop controller can be shown as

$$E_h = E^* - n_h P_h \tag{21}$$

$$\omega_h = \omega^* - m_h Q_h \tag{22}$$

where $P_h$ and $Q_h$ are the calculated values of active power and reactive power under the *hth* harmonic frequency; $n_h$ and $m_h$ are the corresponding *hth* harmonic droop coefficients; $E_h$ is the rms of the *hth* harmonic voltage, and the $\omega_h$ is the *hth* harmonic voltage angle frequency. The amplitude and angular frequency of specific harmonic voltage can be eliminated by this control strategy, and the reference value of harmonic voltage on the *dq* axis can be obtained through voltage synthesis and coordinate transformation. The modulated wave is used to turn on and turn off the inverter switch tube so as to produce appropriate output voltage, so the PCC harmonic voltage can be suppressed effectively.

### C. NEGATIVE SEQUENCE VOLTAGE CONTROL STRATEGY

The output voltage of the inverter is unbalanced when the load is not balanced. According to the theorem of symmetric component method, the output voltage of the inverter can be equivalent to the superposition of the positive sequence component and the negative sequence component of the fundamental wave.

In the *dq* coordinate system, the positive component of the fundamental wave is DC component, and the negative sequence component is the AC component o with a frequency of $2\omega$ while the whole system is stable. One of the major reasons that the negative sequence component leads to the asymmetric voltage. Therefore, as long as the negative sequence is suppressed to 0, the three-phase symmetrical voltage can be output.

The reference value of the negative sequence compensation is calculated as follows (23) and (24):

$$\begin{aligned}\begin{bmatrix} u_{d5} \\ u_{q5} \\ u_{05} \end{bmatrix} &= T_{N5} \begin{bmatrix} u_{a5} \\ u_{b5} \\ u_{c5} \end{bmatrix} \\ &= \frac{2}{3} \begin{bmatrix} -\cos 5\omega t & -\cos(5\omega t+\frac{2\pi}{3}) & -\cos(5\omega t-\frac{2\pi}{3}) \\ \sin 5\omega t & \sin(5\omega t+\frac{2\pi}{3}) & \sin(5\omega t-\frac{2\pi}{3}) \\ 1/\sqrt{2} & 1/\sqrt{2} & 1/\sqrt{2} \end{bmatrix} \\ &\quad \cdot \begin{bmatrix} U_5 \sin 5\omega t \\ U_5 \sin(5\omega t+\frac{2\pi}{3}) \\ U_5 \sin(5\omega t-\frac{2\pi}{3}) \end{bmatrix} \\ &= \begin{bmatrix} 0 \\ U_5 \\ 0 \end{bmatrix} \end{aligned} \tag{23}$$

$$\begin{aligned}\begin{bmatrix} u_{d1N} \\ u_{q1N} \\ u_{01N} \end{bmatrix} &= T_{N1} \begin{bmatrix} u_{a1} \\ u_{b1} \\ u_{c1} \end{bmatrix} \\ &= \frac{2}{3} \begin{bmatrix} \cos \omega t & \cos(\omega t+\frac{2\pi}{3}) & \cos(\omega t-\frac{2\pi}{3}) \\ -\sin \omega t & -\sin(\omega t+\frac{2\pi}{3}) & -\sin(\omega t-\frac{2\pi}{3}) \\ 1/\sqrt{2} & 1/\sqrt{2} & 1/\sqrt{2} \end{bmatrix} \\ &\quad \cdot \begin{bmatrix} U_1 \sin \omega t \\ U_1 \sin(\omega t-\frac{2\pi}{3}) \\ U_1 \sin(\omega t+\frac{2\pi}{3}) \end{bmatrix} \\ &= \begin{bmatrix} -U_1 \sin 2\omega t \\ U_1 \cos 2\omega t \\ 0 \end{bmatrix} \end{aligned} \tag{24}$$

Therefore, the reference value of the negative sequence compensation is (25)

$$\begin{bmatrix} u_{dN}^* \\ u_{qN}^* \end{bmatrix} = \begin{bmatrix} -U_1 \sin 2\omega t \\ U_1 \cos 2\omega t \end{bmatrix} \tag{25}$$

### D. A SECONDARY BALANCE CONTROL STRATEGY

The traditional droop control can realize automatic regulation of P/f and Q/V, but the essence of which is a kind of deviating regulation. Considering the addition of the virtual impedance will increase the degree of deviation, which is harmful to the voltage stability. Harmonic suppression control strategy and unbalanced suppression control strategy are more demanding for stability. Therefore, a secondary balance control strategy is added to stabilize the output voltage of converters, as well as improve the stability of frequency, the compensation frequency and voltage of this strategy can be derived by formula (26) and formula (27):

$$\delta f = k_{p\omega}(f^* - f) + k_{i\omega} \int (f^* - f)dt \tag{26}$$

$$\delta U = k_{pE}(U^* - U) + k_{iE} \int (U^* - U)dt \tag{27}$$

where $f^*$ and $f$ are rated frequency and operational frequency of the microgrid; $U^*$ and $U$ are rated voltage and operational voltage. The frequency compensation signal $\delta f$ and voltage compensation signal $\delta U$ obtained from the secondary balance controller are sent to each micro source, then the droop curves of micro sources will turn to be appropriate translations. Although the deviation from the primary control can be removed by the secondary control, the accurate power distribution will be decreased. It is impossible to eliminate the error $\Delta Q$ of power distribution.

For this reason, this paper proposes modified secondary control method for adjusting the frequency and voltage to bear the proportion of load power. Firstly, the MGCC calculates the proportion of the load based on the actual operating conditions and capacity of all the $n$ micro-sources, that is, the load distribution factor $k_i$.

$$k_i = \frac{S_i}{\sum_{i=1}^{n} x_i S_i} \tag{28}$$

Which $x_i$ indicates the operating status of the $i$th inverter. If it is out of service, $x_i$ will be taken 0, otherwise $x_i = 1$. $S_i$ is the capacity of each micro source. Then, the reference value $Q_i^*$ of the reactive power of each micro-source is calculated according to the following formula:

$$\begin{aligned} \frac{Q_i^*}{\sum Q_i} &= k_i = \frac{S_i}{\sum_{i=1}^{n} x_i S_i} \\ Q_i^* &= k_i \sum Q_i \end{aligned} \tag{29}$$

The reference value $Q_i^*$ of the reactive power is subtracted by the actual reactive power, the result value will be transmitted to the local micro-source controller, which go through the PI regulator, the command signal is superimposed on the secondary voltage control signal and the micro source droop curve is translated.

$$\delta U_i = (k_{pE} + \frac{k_{iE}}{s})(U^* - U) + (k_{ps} + \frac{k_{is}}{s})(k_i \sum Q_i - Q_i) \tag{30}$$

where $Q_i$ is the reactive power that the micro-source actually outputs.

Until now not only the reactive power can be distributed accurately, but also the stability of voltage and frequency can be improved effectively, hence the combination of adaptive virtual impedance drooping control, fractional frequency Harmonic drooping control, negative sequence voltage control and secondary balance control strategy in fundamental frequency is achieved completely.

## IV. STABILITY ANALYSIS OF THE MULTI-CONVERTER PARALLEL SYSTEM AFTER INTRODUCING THE COMPREHENSIVE CONTROL STRATEGY

The detailed derivation of a fundamental droop controller small signal model has been shown in [23], so this paper just focuses on the harmonic droop controller model. The block diagram of the harmonic droop control is shown in Fig. 8.

The harmonic droop control structure contains the harmonic power calculation module, the low pass filter module and the harmonic droop module, which is similar to the

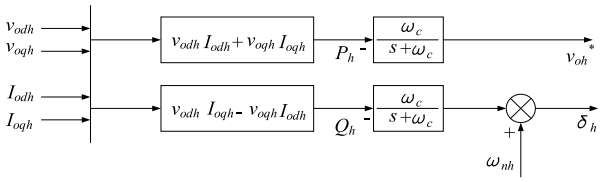


**FIGURE 8.** Harmonic droop control block diagram.

fundamental droop control structure. The small signal model of harmonic power droop controller can be written as the form of state space function, and the expression of state space expression are:

$$\begin{bmatrix} \Delta\dot{\delta}_h \\ \Delta\dot{P}_h \\ \Delta\dot{Q}_h \end{bmatrix} = A_{ph}\begin{bmatrix} \Delta\delta_h \\ \Delta P_h \\ \Delta Q_h \end{bmatrix} + B_{ph}\begin{bmatrix} \Delta i_{ldqh} \\ \Delta v_{odqh} \\ \Delta i_{odqh} \end{bmatrix} + B_{p\omega h}\Delta\omega_{comh} \tag{31}$$

$$\begin{bmatrix} \Delta\omega_h \\ \Delta v^*_{odqh} \end{bmatrix} = \begin{bmatrix} C_{p\omega h} \\ C_{pvh} \end{bmatrix}\begin{bmatrix} \Delta\delta_h \\ \Delta P_h \\ \Delta Q_h \end{bmatrix} \tag{32}$$

Where:

$$A_{ph} = \begin{bmatrix} 0 & 0 & -m_h \\ 0 & -\omega_c & 0 \\ 0 & 0 & -\omega_c \end{bmatrix} B_{p\omega h} = \begin{bmatrix} -1 \\ 0 \\ 0 \end{bmatrix}$$
$$B_{ph} = \begin{bmatrix} 0 & 0 & 0 & 0 & 0 & 0 \\ 0 & 0 & \omega_c I_{odh} & \omega_c I_{oqh} & \omega_c V_{odh} & \omega_c V_{oqh} \\ 0 & 0 & \omega_c I_{oqh} & -\omega_c I_{odh} & -\omega_c V_{oqh} & \omega_c V_{odh} \end{bmatrix}$$
$$C_{p\omega} = \begin{bmatrix} 0 & 0 & -m_h \end{bmatrix} C_{pvh} = \begin{bmatrix} 0 & -n_h & 0 \\ 0 & 0 & 0 \end{bmatrix} \tag{33}$$

where $v_{odh}$ and $v_{oqh}$ represent the output harmonic voltages of inverter in $dq$ coordinate system; $i_{odh}$ and $i_{oqh}$ represent the output harmonic currents of inverter in dq coordinate system; the $P_h$ is the active power of the $hth$ harmonic; the $Q_h$ is the $hth$ harmonic reactive power; $\omega_c$ represents the cut-off frequency of the low pass filter; $m_h$ is the reactive power drooping coefficient of the $hth$ harmonic; $n_h$ is the active power drooping coefficient of the $hth$ harmonic; $\omega_h$ is the $hth$ harmonic angular frequency; $\omega_{\mathrm{comh}}$ is the common angular frequency in the $hth$ harmonic coordinate system; $\delta_h$ is the $hth$ harmonic angle.

The linearization of harmonic drooping voltage loop is the same as fundamental linearization, and linearizing the differential equation of the line and load, the state space equation of the line and load can be obtained [22].

The state space model of the fundamental droop control strategy in the multi-inverter-based microgrid is:

The small signal state space model of the fundamental wave droop control strategy in the microgrid can be shown as follow (34) and (35):

$$\Delta\dot{x}_{\mathrm{mg}} = A_{\mathrm{mg}}\Delta x_{\mathrm{mg}} \tag{34}$$
$$\Delta x_{\mathrm{mg}} = \begin{bmatrix} \Delta\delta & \Delta P & \Delta Q & \Delta\phi_{\mathrm{dq}} & \Delta\gamma_{\mathrm{dq}} \\ \Delta i_{\mathrm{ldq}} & \Delta v_{\mathrm{odq}} & \Delta i_{\mathrm{odq}} & \Delta i_{\mathrm{loaddq}} \end{bmatrix} \tag{35}$$

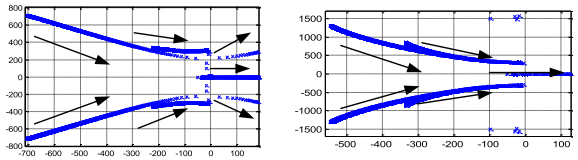

(a) (b)

**FIGURE 9.** (a) The active power coefficient $m_p$ root locus of the fundamental wave; (b) The reactive power coefficient $n_q$ root locus of the fundamental wave.

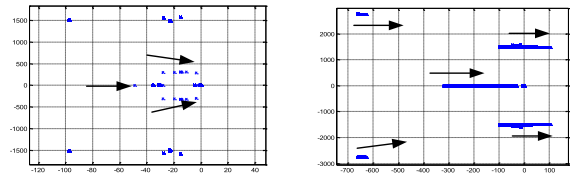

(a) (b)

**FIGURE 10.** (a) The reactive power coefficient $m_{ph}$ root locus of the harmonic wave; (b) The active power coefficient $n_{qh}$ root locus of the harmonic wave.

The small signal state space model of the harmonic wave droop control strategy in microgrid can be shown as follow (36) and (37):

$$\Delta\dot{x}_{\mathrm{mgh}} = A_{\mathrm{mgh}}\Delta x_{\mathrm{mgh}} \tag{36}$$
$$\Delta x_{\mathrm{mgh}} = \begin{bmatrix} \Delta\delta_h & \Delta P_h & \Delta Q_h\Delta\phi_{\mathrm{dq}} & \Delta i_{\mathrm{ldqh}} \\ & & \Delta v_{\mathrm{odqh}} & \Delta i_{\mathrm{odqh}} & \Delta i_{\mathrm{loaddqh}} \end{bmatrix} \tag{37}$$

The small signal state space model of the negative sequence droop control strategy in microgrid can be shown as follow (38) and (39):

$$\Delta\dot{x}_{\mathrm{mgub}} = A_{\mathrm{mgub}}\Delta x_{\mathrm{mgub}} \tag{38}$$
$$\Delta x_{\mathrm{mgub}} = \begin{bmatrix} \Delta\delta_{ub} & \Delta P_{ub} & \Delta Q_{ub} & \Delta\phi_{\mathrm{dqub}} & \Delta i_{\mathrm{ldqub}} \\ & & \Delta v_{\mathrm{odqub}} & \Delta i_{\mathrm{odqub}} & \Delta i_{\mathrm{loaddqub}} \end{bmatrix} \tag{39}$$

The state space model of the harmonic droop control strategy in the multi-inverter-based microgrid is:

$$\Delta\dot{x}_{\mathrm{mga}} = A_{\mathrm{mga}}\Delta x_{\mathrm{mga}} \tag{40}$$
$$\Delta\dot{x}_{\mathrm{mga}} = \begin{bmatrix} \Delta\dot{x}_{\mathrm{mg}} \\ \Delta\dot{x}_{\mathrm{mgh}} \\ \Delta\dot{x}_{\mathrm{mgub}} \end{bmatrix} \quad \Delta x_{\mathrm{mga}} = \begin{bmatrix} \Delta x_{\mathrm{mg}} \\ \Delta x_{\mathrm{mgh}} \\ \Delta x_{\mathrm{mgub}} \end{bmatrix} \tag{41}$$
$$A_{\mathrm{mga}} = \begin{bmatrix} A_{\mathrm{mg}} & 0 & 0 \\ 0 & A_{\mathrm{mgh}} & 0 \\ 0 & 0 & A_{\mathrm{mgub}} \end{bmatrix} \tag{42}$$

where $x_{mg}$ is the state variable under fundamental frequency; $i_{loaddq}$ is a load fundamental current; $A_{mg}$ is a fundamental state matrix; $x_{mgh}$ is the state variable under the $hth$ harmonic frequency; $i_{loadqdh}$ is the $hth$ harmonic load current; $A_{mgh}$ is the $hth$ harmonic state matrix; $i_{loaddqub}$ is the negative sequence load current; $A_{mgub}$ is the negative sequence state matrix; $x_{mga}$ is the comprehensive state variable under all frequencies; $A_{mga}$ is the comprehensive state matrix.

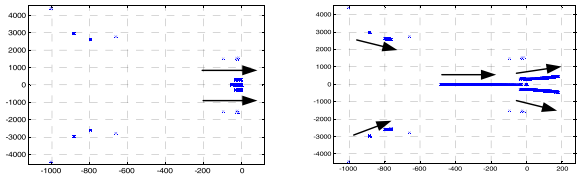

**FIGURE 11.** (a) The reactive power coefficient $m_{pub}$ root locus of Negative sequence component; (b) The active power coefficient $n_{qub}$ root locus of Negative sequence component.

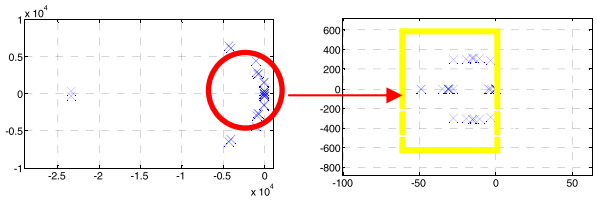

**FIGURE 12.** (a) The root locus of the parameters used in the experiment; (b) Part of the A graph is magnified.

The stability analysis of the proposed comprehensive strategy is shown in Figs. 9-12.

From Fig. 9 (a), when the active power drooping coefficient $m_p$ varies from 0 to 1, the overall trend of the system root locus move towards the right side with the increase of $m_p$, and reaches the right half plane eventually, the system gradually loses its stability. Namely, the system becomes instability if the $m_p$ is too large. From Fig.9 (b), when the reactive power drooping coefficient $n_q$ varies from 0 to 1, the overall trend of the system root locus move towards the right side with the increase of $n_q$, and reaches the right half plane eventually, the system gradually loses its stability. Namely, the system also becomes instability if $n_q$ is too large.

From Fig.10 (a), when $m_{ph}$ varies from 0 to 1, the overall trend of the system root locus move towards the right side with the increase of $m_{ph}$, the system stability is weakened gradually. The Fig.11 (a) is the same effect as Fig.10 (a). From Fig.10 (b), when $n_{qh}$ varies from 0 to 1, the overall trend of the system root locus move towards the right side with the increase of $n_{qh}$, and reaches the right half plane eventually, t the system stability is also weakened gradually. The Fig.11 (b) is the same effect as Fig. 10 (b)

Fig. 12 shows the root locus of the proposed multi-inverter-based microgrid system with comprehensive control strategy, which proves that all eigenvalues are located in the left half plane, namely the system controlled by the comprehensive strategy is stable.

## V. SIMULATION AND EXPERIMENTAL ANALYSIS

### A. SIMULATION ANALYSIS

Simulations are built in MATLAB2014B, and the 5th, 7th harmonics components are injected in the model. The inverter output phase voltage amplitude is 311V, and the frequency is 50Hz.In order to verify the effectiveness of the proposed

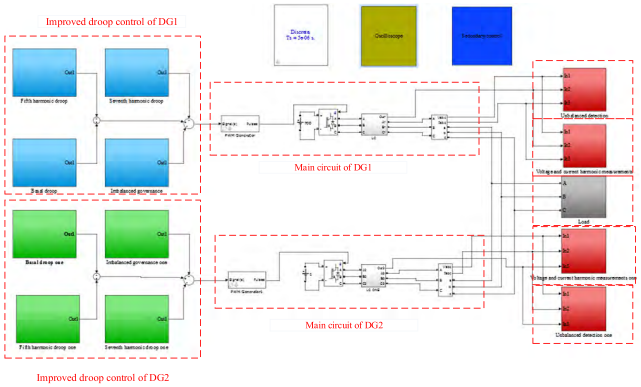


**FIGURE 13.** The simulation model in MATLAB2014B.

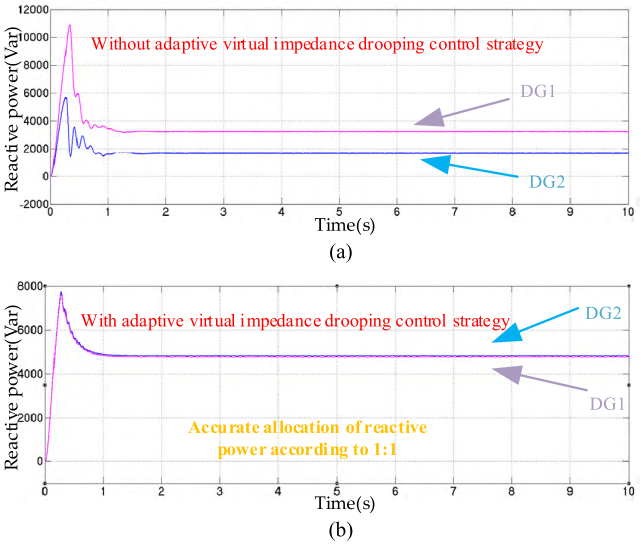


**FIGURE 14.** (a) Reactive power allocation of DG1 and DG2 without control strategy; (b) Reactive power allocation of DG1 and DG2 with control strategy.

control strategy, the simulation analysis is carried out according to the following steps:

*Step 1:* Adaptive virtual impedance drooping control strategy. The proportional distribution problem of reactive power between micro sources will be verified.

*Step 2:* Fractional frequency Harmonic drooping control strategy. The effect of eliminating the 5th and 7th harmonics will be verified.

*Step 3:* Negative sequence voltage control strategy. The decrease of the negative sequence voltage content will be proved.

*Step 4:* A secondary balance control strategy. The precision adjustment of voltage and frequency will be proved will be proved. At the same time, the effectiveness of the comprehensive control strategy is verified.

The simulation model in MATLAB2014B is shown in Fig. 13.

The simulation parameters are shown in TABLE I:

*Simulation 1:* Adaptive virtual impedance drooping control strategy.

**TABLE 1. Information of simulation parameters.**

| Name | Symbol | Value |
|---|---|---|
| Main circuit | $L_f$ | $0.6\times10^{-3}$H |
| Main circuit | $R_f$ | $1\times10^{-2}\Omega$ |
| Main circuit | $U_{ab}$ | 700V |
| Main circuit | $L_{line}$ | $2.8\times10^{-3}$ H |
| Main circuit | $R_{line}$ | $4.28\times10^{-2}$ Ω |
| Virtual impedance | $R_{ref1}$ | 2.14×10-3 Ω |
| Virtual impedance | $R_{ref2}$ | 2.14×10-3 Ω |
| Virtual impedance | $X_{ref1}$ | $1.284\times10^{-1}$ |
| Virtual impedance | $X_{ref2}$ | $1.284\times10^{-1}$ |
| Fundamental wave droop | $f^*$ | 50Hz |
| Fundamental wave droop | $U^*$ | 311V |
| Fundamental wave droop | $m1{:}m2$ | 1:1 |
| Fundamental wave droop | $m1$ | $1\times10^{-5}$ |
| Fundamental wave droop | $m2$ | $1\times10^{-5}$ |
| Fundamental wave droop | $n1{:}n2$ | 1:1 |
| Fundamental wave droop | $n1$ | $3\times10^{-5}$ |
| Fundamental wave droop | $n2$ | $3\times10^{-5}$ |
| Fundamental wave droop | $k_{up}$ | 10 |
| Fundamental wave droop | $k_{ui}$ | 100 |
| Fundamental wave droop | $k_{ip}$ | 5 |
| Harmonic wave droop | $f^*$ | 0 Hz |
| Harmonic wave droop | $U^*$ | 0V |
| Harmonic wave droop | $m1{:}m2$ | 1:1 |
| Harmonic wave droop | $m1$ | $-1.361\times10^{-2}$ |
| Harmonic wave droop | $m2$ | $-1.361\times10^{-2}$ |
| Harmonic wave droop | $n1{:}n2$ | 1:1 |
| Harmonic wave droop | $n1$ | $2.609\times10^{-2}$ |
| Harmonic wave droop | $n2$ | $-2.609\times10^{-2}$ |
| Harmonic wave droop | $k_{up}$ | 10 |
| Harmonic wave droop | $k_{ui}$ | 50 |
| Negative sequence droop | $f^*$ | 0 Hz |
| Negative sequence droop | $U^*$ | 0V |
| Negative sequence droop | $m1{:}m2$ | 1:1 |
| Negative sequence droop | $m1$ | $-1.361\times10^{-2}$ |
| Negative sequence droop | $m2$ | $-1.361\times10^{-2}$ |
| Negative sequence droop | $n1{:}n2$ | 1:1 |
| Negative sequence droop | $n1$ | $2.609\times10^{-2}$ |
| Negative sequence droop | $n2$ | $-2.609\times10^{-2}$ |
| Negative sequence droop | $k_{up}$ | 10 |
| Negative sequence droop | $k_{ui}$ | 2 |

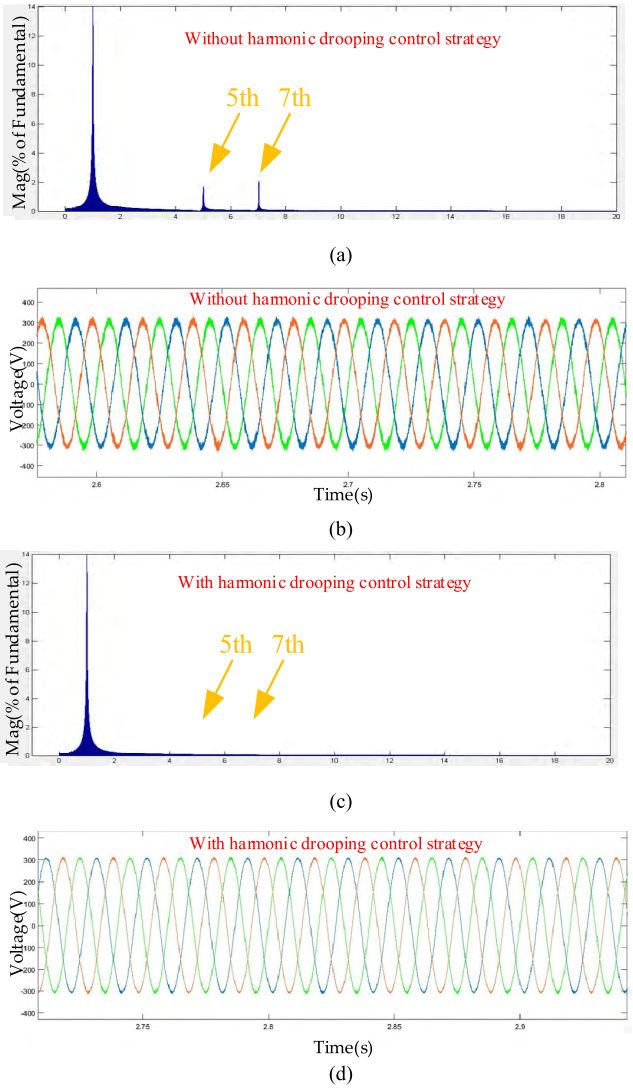


**FIGURE 15.** (a) FFT of voltage without the harmonic droop control strategy; (b) Voltage waveform without the harmonic droop control strategy; (c) FFT of voltage without the harmonic droop control strategy; (d) Voltage waveform with the harmonic droop control strategy.

*Simulation 1 conditions:* The capacity of the two inverters is the same, and the impedance of the line is different. The results of the simulation are shown in Fig. 14.

In Fig. 14(a), it can be seen that the reactive power of the DG1 and DG2 inverters is not proportionately distributed, and the circulation is easily formed between the inverters. In Fig. 14(b), it can be seen that the reactive power distribution is improved effectively after the virtual impedance is added, and the reactive power distribution is more accurate.

*Simulation 2:* Fractional frequency Harmonic drooping control strategy.

*Simulation 2:* The capacity of the two inverters is the same, and the impedance of the line is different. The 5th and 7th harmonics are injected into the system. The results of the simulation are shown in Fig. 15.

From Fig. 15(a) and (b), it can be seen that there are 5th and 7th harmonics in the system, and the voltage waveform of the PCC point has been distorted. From Fig. 15(c) and (d), the voltage waveform is obviously improved after adding fractional frequency harmonic drooping control strategy. At the same time, it is found through FFT that 5th and 7th harmonics are almost eliminated after the addition of the fractional frequency harmonic drooping control strategy, which proves the effectiveness of the harmonic control strategy.

*Simulation 3:* Negative sequence voltage control strategy

*Simulation 3:* The capacity of the two inverters is the same, and the impedance of the line is different. The 5th and 7th harmonics are injected into the system. Load resistance $R_1 = R_2 = 100\Omega, R_3 = 10\Omega$. The results of the simulation are shown in Fig. 16.

In Fig. 16(a), it can be seen that the value of negative sequence voltage is 9.24V. In other words, value of unbalance factor is 4.2% beyond the standard value. The waveform of voltage has been distorted. In Fig. 16(b), it can be seen that the value of the negative sequence voltage is reduced from

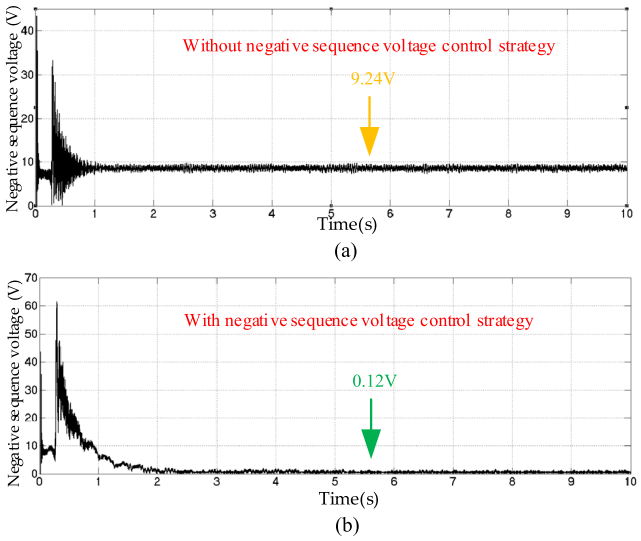


**FIGURE 16.** (a) The value of negative sequence voltage without negative sequence voltage droop control strategy; (b) The value of negative sequence voltage with negative sequence voltage droop control strategy.

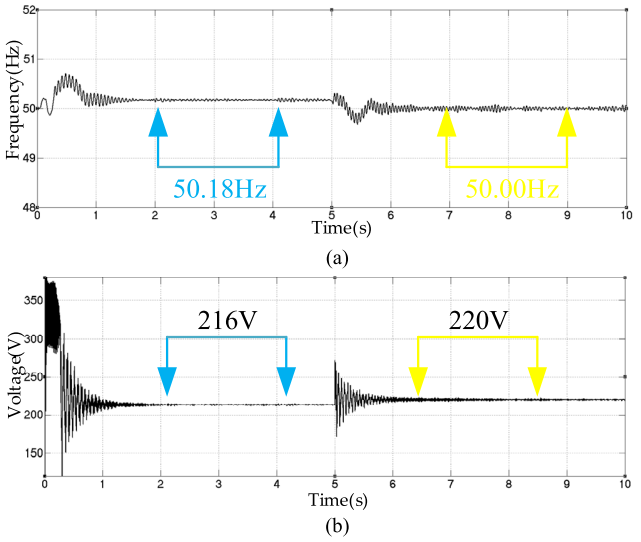


**FIGURE 17.** (a) frequency; (b) The value of PCC voltage.

9.24V to 0.12V with negative sequence voltage droop control strategy. The value of unbalance factor is 0.05%, and this value meets the standard requirements. The value of negative sequence voltage is reduced and the problem of unbalanced three-phase voltage is eliminated.

*Simulation 4:* A secondary balance control strategy.

*Simulation 4:* The capacity of the two inverters is the same, and the impedance of the line is different. The 5th and 7th harmonics are injected into the system. Load resistance $R_1 = R_2 = 100\Omega, R_3 = 10\Omega$. The results of the simulation are shown in Fig. 16. All the control strategies of Simulation 1, Simulation 2, and Simulation 3 run. The secondary balance is not activated during 0-5s, and it is activated during 5-10s. The results of the simulation are shown in Fig. 17.

**TABLE 2.** The effects of control strategy simulation.

| Simulation effect | Simulation1 | Simulation2 | Simulation 3 | Simulation4 |
|---|---|---|---|---|
| Reactive power distribution | YES | NO | NO | YES |
| Harmonic suppression | NO | YES | YES | YES |
| Unbalance suppression | NO | NO | YES | YES |
| Voltage and frequency stabilization | NO | NO | NO | YES |

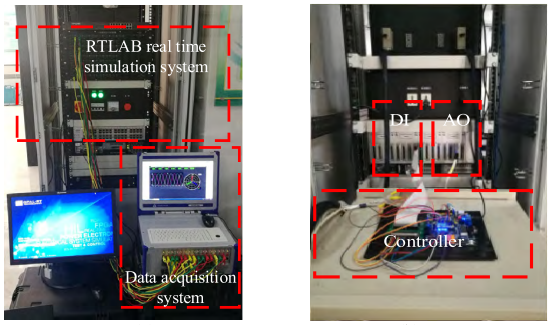


**FIGURE 18.** The hardware-in-loop (front); (b) The hardware-in-loop (back).

From Fig. 17 (a) and (b), it can be seen that frequency deviates from the standard value, and the voltage of PCC is 216V less than 220V during 0-5s. A secondary balance control strategy control strategy is activated at 5s. The frequency is fast back to 50Hz, and the voltage of PCC is rapidly rising to 220V. It can be seen that the effect of A secondary balance control strategy is effective.

According to these four simulations, it can be seen that the comprehensive strategy this paper proposed can guarantee the accurate distribution of active power and reactive power between micro sources. The 5th, 7th harmonics components can be effectively suppressed. Meanwhile. The unbalance of PCC voltage can be effectively controlled. The voltage of PCC and frequency can be stabilized at 220V and 50Hz. The effects of these four simulations are shown in TABLE.II

### B. EXPERIMENTAL ANALYSIS

In this paper, the experimental research is carried out in the Microgrid Simulation Laboratory of Electric Power Research Institute of Liaoning Electric Power Co., Ltd. of State Grid. Simulation models are built in the real time simulation platform RTLAB, and the hardware-in-loop(HIL) is formed. the nonlinear load is added in the experiment, and the data acquisition system DEWE5000 is used to record the waveform and data.

Experimental conditions in this paper: the two micro sources are DG1 and DG2, the active power reference value $P_{ref} = 20$kW, and the reactive power reference value $Q_{ref} = 0$kVar. The active power of the linear load is 20kW,

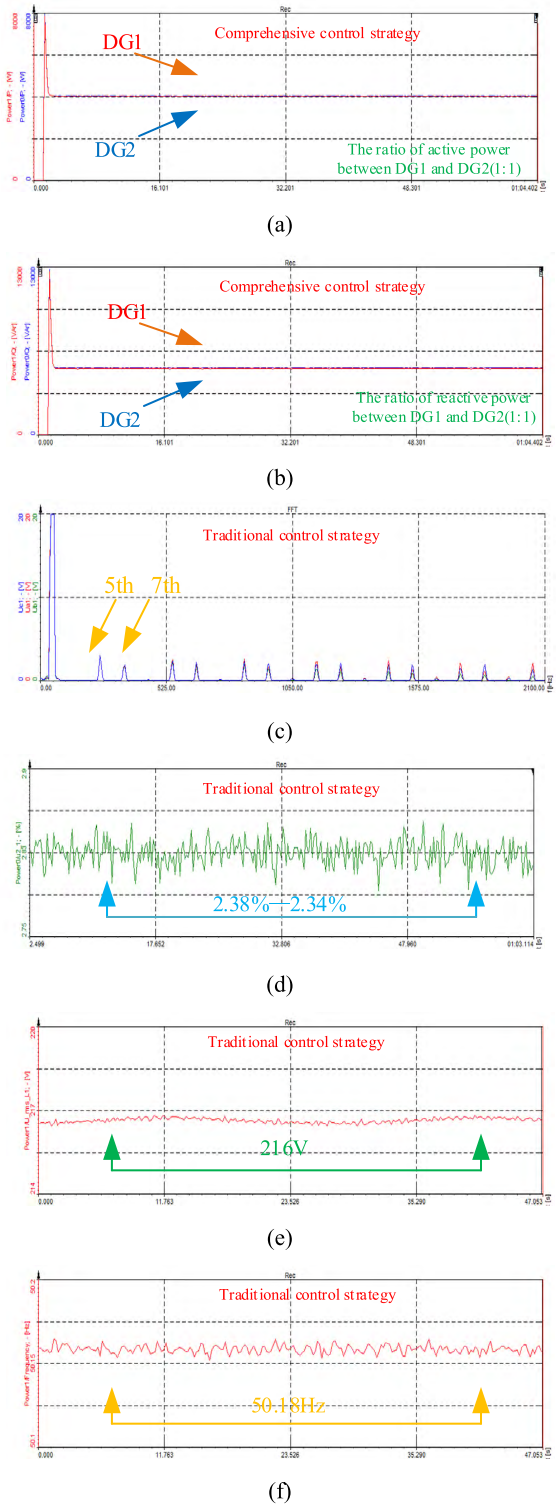


**FIGURE 19.** (a) Active power distribution between DG1 and DG2; (b) Reactive power distribution between DG1 and DG2; (c) FFT of voltage with traditional control strategy; (d) The value of negative sequence voltage with traditional control strategy; (e) The value of PCC voltage; (f) frequency.

and the reactive power is 0kW. The active power of the nonlinear load is 20kW, the reactive power 0KW. Line resistance of DG1 is $R_1 = 1.07 * 10^{-2}\Omega$, inductance $L_1 = 0.7 * 10^{-3}$H.

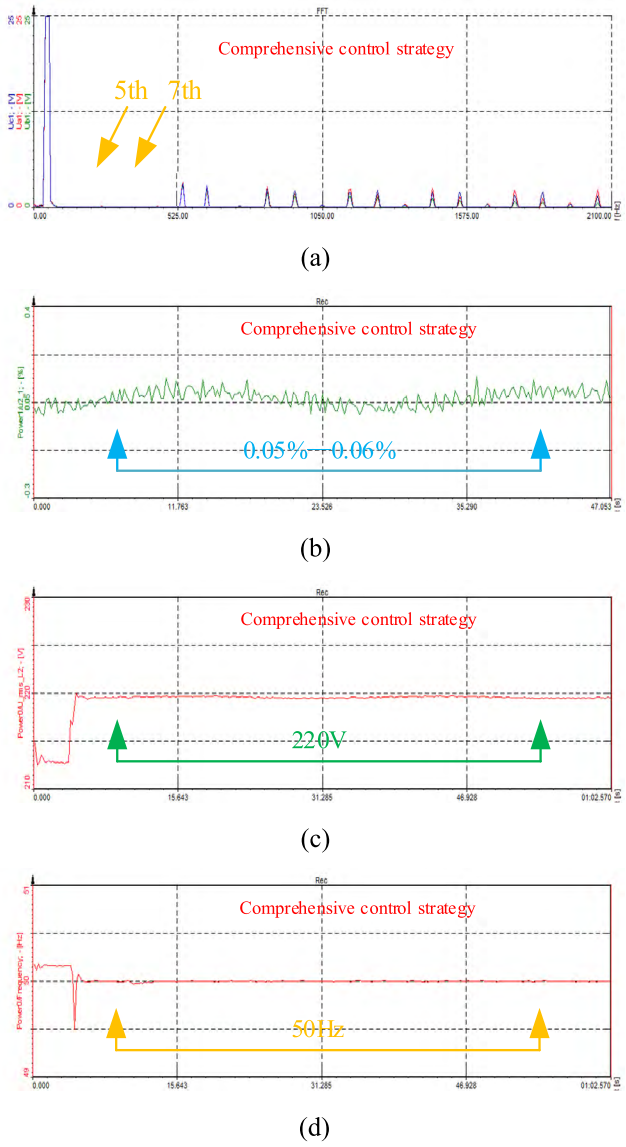


**FIGURE 20.** (a) FFT of voltage with comprehensive control strategy; (b) The value of negative sequence voltage with control strategy; (c) The value of PCC voltage; (d) frequency.

Line resistance of DG2 is $R_2 = 4.28 * 10^{-2}\Omega$, inductance $L_2 = 2.8 * 10^{-3}$H. The experimental environment is shown in Fig. 18.

*Experimental 1:* Fundamental wave adaptive virtual impedance drooping control strategy: linear load + nonlinear load + unbalance load. The results of the experimental are shown in Fig. 19.

In Fig. 19(a) and 19(b), it can be seen that fundamental wave adaptive virtual impedance drooping control strategy can realize the accurate allocation of active power and reactive power between micro sources. Compared with the traditional droop control, the circulation problem caused by the unbalance of the reactive power distribution between the micro sources is reduced. However, the control strategy cannot suppress harmonic and the negative sequence component

of voltage. for nonlinear load and unbalanced load when the nonlinear load and unbalanced load in the system. In Fig. 19(c), the existence of 5th, 7th, 11th, and 13th harmonics in the system. In Fig. 19(d), the unbalance factor of voltage beyond the standard. At the same time, the voltage and frequency cannot be accurately stabilized at 220V and 50Hz

*Experimental 2:* Comprehensive control strategy: linear load + nonlinear load + unbalance load. The results of the experimental are shown in Fig. 20.

In Fig. 20(a), it can be seen that the 5th and 7th harmonics are eliminated. This method can be widely used for the elimination of any harmonics. The voltage unbalance is reduced to about 0.05%, which meets the requirements of the standard. From Fig. 20(c) and 20(d), the voltage and frequency can be accurately stabilized at 220V and 50Hz. The comprehensive control strategy is effective, and the stability of the system is improved.

## VI. CONCLUSION

This paper proposes a comprehensive strategy for accurate power distribution, harmonic suppression, voltage negative sequence component suppression, and stability improvement of multi-inverter-based microgrid, with the combination of virtual impedance droop control and secondary power balance control, the active and reactive can be distributed accurately, meanwhile the stability of voltage and frequency are obviously improved, next a harmonic suppression control strategy is introduced to suppress harmonic components in microgrid. Furthermore, small signal analysis is used to analyze the stability of the proposed multi-converter parallel system after introducing the comprehensive theory. The simulation and experimental of results certify that proposed the strategy has great performance on accurate reactive power distribution, harmonic suppression, voltage negative sequence component suppression, stability improvement.

## REFERENCES

[1] Y. Li, B. Feng, G. Li, J. Qi, D. Zhao, and Y. Mu, "Optimal distributed generation planning in active distribution networks considering integration of energy storage," *Appl. Energy*, vol. 210, pp. 1073–1081, Jan. 2018.

[2] G. Benysek and M. Pasko, *Power Theory and Power Quality Management*, 1st ed. Beijing, China: China Machine Press, Oct. 2013.

[3] Z. Jianhua and H. Wei, *Microgrid Operation Control and Protection Technology*, 1st ed. Beijing, China: China Electric Power Press, Jul. 2010.

[4] Y. Li, Y. Li, G. Li, D. Zhao, and C. Chen, "Two-stage multi-objective OPF for AC/DC grids with VSC-HVDC: Incorporating decisions analysis into optimization process," *Energy*, vol. 147, pp. 286–296, Mar. 2018.

[5] W. Jibiao, C. Qihong, and L. Li, "Grid connected inverter control of three phase voltage unbalance compensation in micro grid," *Autom. Electr. Power Syst.*, vol. 41, no. 8, pp. 38–44, 2017.

[6] G. Weinong and C. Jian, "Research on inverter digital double loop control technology based on state observer," *Chin. Soc. Elect. Eng.*, vol. 22, no. 9, pp. 64–68, 2002.

[7] K. Xuejuan, W. Jingjiang, and P. Li, "Waveform control of three phase voltage source inverter based on internal model theory," *Chin. Soc. Elect. Eng.*, vol. 23, no. 7, pp. 67–70, 2003.

[8] J. M. Guerrero, J. C. Vasquez, J. Matas, M. Castilla, and L. G. de Vicuna, "Control strategy for flexible microgrid based on parallel line-interactive UPS systems," *IEEE Trans. Ind. Electron.*, vol. 56, no. 3, pp. 726–736, Mar. 2009.

[9] W. Yingchang, W. Yi, and X. Haojiang, "Harmonic current suppression of photovoltaic grid connected inverter," *Power Electron. Technol.*, vol. 47, no. 1, pp. 46–85, 2013.

[10] B. Dan, C. Zhikai, and P. Li, "Research on unbalanced load of three phase inverter," *Autom. Electr. Power Syst.*, vol. 28, no. 9, pp. 53–57, 2004.

[11] X.-B. Yang, W.-Y. Wu, and H. Shen, "Adaptive three dimensional space vector modulation in abc coordinates for three phase four wire split capacitor converter," in *Proc. IEEE Trans. Power Electron. Motion Control Conf.*, Aug. 2009, pp. 1–5.

[12] K.-H. Kim, N.-J. Park, and D.-S. Hyun, "Advanced synchronous reference frame controller for three-phase UPS powering unbalanced and nonlinear loads," in *Proc. IEEE Trans. Power Electron. Specialists Conf.*, Jun. 2005, pp. 1699–1704.

[13] S. El-Barbari and W. Hofmann, "Digital control of a three phase 4 wire 782 PWM inverter for PV applications," in *Proc. IEEE Ind. Electron. Soc. Conf. (IECON)*, 2000.

[14] S. Emamian, M. Hamzeh, H. Karimi, A. Bakhshai, and K. Paridari, "Robust decentralized voltage control of an islanded microgrid under unbalanced and nonlinear load conditions," in *Proc. IEEE Trans. Int. Conf. Ind. Technol.*, Feb. 2013, pp. 1825–1830.

[15] K. Paridari, M. Hamzeh, S. Emamian, H. Karimi, and A. Bakhshai, "A new decentralized voltage control scheme of an autonomous microgrid under unbalanced and nonlinear load conditions," in *Proc. IEEE Trans. Int. Conf. Ind. Technol.*, Feb. 2013, pp. 1812–1817.

[16] C. Min, "Research on inverter characteristics under nonlinear load," Ph.D. dissertation, College Elect. Eng., Zhejiang Univ., Hangzhou, China, 2006.

[17] P. Jin, Y. Li, G. Li, Z. Chen, and X. Zhai, "Optimized hierarchical power oscillations control for distributed generation under unbalanced conditions," *Appl. Energy*, vol. 194, pp. 343–352, May 2017.

[18] D. C. Patel, R. R. Sawant, and M. C. Chandorkar, "Three-dimensional flux vector modulation of four-leg sine-wave output inverters," *IEEE Trans. Ind. Electron.*, vol. 57, no. 4, pp. 1261–1269, Apr. 2010.

[19] H. Qunhai, K. Li, and T. Qisheng, "Control principles of micro-source inverters used in microgrid," *Chin. Soc. Elect. Eng.*, vol. 30, no. 15, pp. 10–15, 2010.

[20] R. Biying, Z. Yinrong, S. Xiangdong, and Y. Hui, "Combined three—Phase inverter control based on improved droop control strategy under unbalanced load," *Grid Technol.*, vol. 40, no. 4, pp. 1163–1168, Apr. 2016.

[21] H. Qunhai and L. Ningning, "Micro-source inverter with mixed load control in microgrid," *Trans. China Electrotech. Soc.*, vol. 28, no. 2, pp. 270–277, 2013.

[22] C. M. Tu, Y. Yang, and F. Xiao, "The output side power quality control strategy for microgrid main inverter under nonlinear load," *Trans. China Electrotech. Soc.*, vol. 32, no. 22, pp. 53–62, 2017.

[23] H. Moussa, A. Shahin, J.-P. Martin, B. N.-Mobarakeh, S. Pierfederici, and N. N. Moubayed, "Harmonic power sharing with voltage distortion compensation of droop controlled islanded microgrids," *IEEE Trans. Smart Grid*, to be published, doi: 10.1109/TSG.2017.2687058.

**HENAN DONG** was born in Chifeng, China, in 1986. He received the M.S. degree in power electronics and drives from the Shenyang University of Technology, Shenyang, China, in 2013, where he is currently pursuing the Ph.D. degree with the School of Institute of Electrical Engineering. His research interests include the key technology and power quality of microgrid.

From 2013 to 2018, he was a Senior Engineer with Liaoning Electric Power Company Electric Power Research Institute.

**SHUN YUAN** was born in Shenyang, China, in 1963. He received the Ph.D. degree from Xi'an Jiaotong University, Xi'an, in 1993.

From 2016 to 2018, he was the Director of the Power Qualification Management Center, National Energy Administration. He is currently a Professor and a Doctorate Tutor. His research interests include the key technology of microgrid and high-voltage switches.

**ZIJIAO HAN** was born in Tongliao, China, in 1988. She received the B.S. degree in electrical engineering from Zhejiang University, Hangzhou, in 2011, and the M.S. degree in power system and automation from Tsinghua University, Beijing, in 2013.

Her research interests include key technology of UHV and stability analysis of power system.

From 2013 to 2017, she was a Senior Engineer with Liaoning Electric Power Company Electric Power Research Institute.

From 2017 to 2018, she was a Senior Engineer with Liaoning Electric Power Company.

**XIYING DING** was born in Shenyang, China, in 1963. She received the B.S. degree from the School of Industrial Automation, Northeast University, and the M.S. and Ph.D. degrees from the School of Electrical Engineering, Shenyang University of Technology, Shenyang.

Since 1987, she has been with the School of Electrical Engineering, Shenyang University of Technology. She is currently a Professor with the Institute Industrial Automation, Shenyang University of Technology. Her research interests include the development of electric vehicle and performance and control of microgrid.

**SHAOHUA MA** received the bachelor's and Ph.D. degrees in electrical engineering from the Shenyang University of Technology in 1988 and 2008, respectively. She has been the Head of the Department of Electrical Machinery since 2014. She is currently a Professor with the School of Electrical Engineering, Shenyang University of Technology. Her research interests include renewable energy generation, intelligent electrical apparatus, and advanced digital control technique and power electronics applications in power systems.

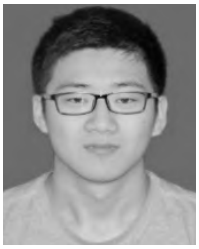

**XIANGYU HAN** was born in Shenyang, China, in 1994. He received the B.S. degree in automation from the Polytechnic School, Shenyang Ligong University, Shenyang, in 2016. He is currently pursuing the master's degree with the School of Shenyang University of Technology, Shenyang.